

# 振动辅助磁针磁力研磨法对管件焊缝 表面氧化皮的去除实验

程海东, 马小刚, 韩冰, 陈燕, 朱慧宁

(辽宁科技大学, 辽宁 鞍山 114051)

**摘要:** 目的 去除焊接管件焊缝处的氧化皮, 改善焊缝处的应力状态。方法 采用振动辅助磁针磁力研磨法去除导磁材质管件经焊接处理后焊缝表面的氧化皮, 利用超景深电子显微镜观察氧化皮的去除情况; 利用 X 射线能谱分析仪对焊缝表面氧化皮的成分进行分析, 根据氧化皮及管件材料主要元素的占比情况, 分析检测焊缝表面氧化皮是否被完全去除。结果 焊缝表面氧化皮经振动辅助磁针磁力研磨后被完全去除。通过对比振动辅助磁针磁力研磨前后的表面形貌发现, 表面颜色由黑变光亮, 氧化皮得到有效去除。通过 EDS 成分分析可知, 氧化皮的主要成分为 C 元素, 质量分数为 88.62%; 管切面显示基体的主要成分为 Fe 元素, 质量分数为 67.09%。通过振动辅助磁力研磨法去除氧化皮后, 管表面的元素组成与研磨前相比 C 元素降低了 85.52%, Fe 元素增加了 63.06%。表面残余应力由原始的 +17.5 MPa 变为 -186.0 MPa。经研磨后, 氧化皮基本被完全去除。结论 焊缝表面成分的检测结果证实, 从表面形貌分析中得到氧化皮被完全去除的结论是正确的, 同时也表明振动辅助磁针磁力研磨对完全去除焊缝表面的氧化皮具有可行性。

**关键词:** 氧化皮; 振动辅助磁力研磨; 表面形貌; 焊缝; 去除机理

**中图分类号:** TG176    **文献标识码:** A    **文章编号:** 1001-3660(2022)08-0400-08

**DOI:** 10.16490/j.cnki.issn.1001-3660.2022.08.036

## Removal of Oxide Scale on Weld Surface of Pipe Fittings by Vibration Assisted Magnetic Needle Magnetic Grinding

CHENG Hai-dong, MA Xiao-gang, HAN Bing, CHEN Yan, ZHU Hui-ning

(University of Science and Technology Liaoning, Liaoning Anshan 114051, China)

**ABSTRACT:** Magnetic needle magnetic grinding technology, as a kind of surface finishing technology, has the advantages of good flexibility and adaptability. Besides, it can also conduct finishing process on small parts, complex outer surfaces and inner surfaces of pipes. Due to the existence of defects such as oxide scale at the weld joints, the service performance of the parts is

收稿日期: 2021-09-25; 修订日期: 2022-03-10

Received: 2021-09-25; Revised: 2022-03-10

基金项目: 国家自然科学基金 (51775258); 辽宁省自然科学基金重点项目 (20170540458); 精密与特种加工教育部重点实验室基金 (B201703)

**Fund:** National Natural Science Foundation of China (51775258); Natural Science Foundation Plan Key Projects of Liaoning Province (20170540458); Key Laboratory Fund of Ministry of Precision and Special Processing Education (B201703)

作者简介: 程海东 (1996—), 男, 硕士, 主要研究方向为工件表面精密加工技术。

**Biography:** CHENG Hai-dong (1996-), Male, Master, Research focus: precision machining technology of workpiece surface.

通讯作者: 马小刚 (1988—), 男, 硕士, 讲师, 主要研究方向为复杂工件表面特种加工技术。

**Corresponding author:** MA Xiao-gang (1988-), Male, Master, Lecturer, Research focus: special machining technology of complex workpiece surface.

引文格式: 程海东, 马小刚, 韩冰, 等. 振动辅助磁针磁力研磨法对管件焊缝表面氧化皮的去除实验[J]. 表面技术, 2022, 51(8): 400-407. CHENG Hai-dong, MA Xiao-gang, HAN Bing, et al. Removal of Oxide Scale on Weld Surface of Pipe Fittings by Vibration Assisted Magnetic Needle Magnetic Grinding[J]. Surface Technology, 2022, 51(8): 400-407.

seriously affected. This article uses vibration assisted magnetic needle magnetic grinding technology to grind welded pipe fittings, and explores the effect of removing oxide scale on the weld surface and the improvement of the residual stress state, which provides a new method for weld surface treatment.

In order to compare the effects of vibration assisted magnetic needle magnetic grinding and single magnetic needle magnetic grinding on the processing effect, an iron welded pipe with an outer diameter of 35 mm and a wall thickness of 4 mm was selected as the experimental object. It was cut along the axial direction and its original appearance was recorded by a VHX-500 ultra-depth-of-field microscope at the same time. The welded pipe fitting was placed in a magnetic grinding device for testing. The grinding medium were magnetic needles of  $\phi 0.5 \text{ mm} \times 5 \text{ mm}$ , the rotation speed of the magnetic pole plate was 480 r/min, the processing time was 40 minutes, and the amplitude in the vibration assisted magnetic grinding test was  $\pm 3 \text{ mm}$ . By comparing the surface morphology of the inner surface of welded pipe fittings with and without vibration assisted grinding, the effect of vibration assisted magnetic needle magnetic grinding on the processing quality and efficiency under the same processing conditions was explored. In order to explore the effect of oxide scale removal at the weld, the cut surface of the welded pipe was polished to expose the matrix, and the inner wall of the welded pipe before and after processing was analyzed by X-ray energy dispersive spectroscopy (EDS). The element composition was compared with that the matrix element composition to verify whether the oxide scale had completely removed. An X-ray diffractometer was used to detect the residual stress before and after grinding at the weld of the pipe fittings, and the influence of the vibration assisted magnetic needle magnetic grinding method on the stress state of the welded pipe fittings was explored.

Compared with a single magnetic needle magnetic grinding technology, the vibration assisted magnetic needle magnetic grinding technology can effectively improve the grinding efficiency and obtain a better grinding effect. It can be obtained by splitting the component elements. The main components of the welded pipe fitting are composed of C, Cr, Fe, Mo and Si. The content of Fe is the highest at 67.09%. After processing, the surface elements of the pipe are approximately the same as the matrix elements, and the presence of oxide scale cannot be found on the surface morphology either, indicating that the oxide scale has been completely removed. Through the detection of the surface residual stress, it can be seen that the residual stress at the weld has changed from the original tensile stress of 17.5 MPa to the compressive stress of 186.0 MPa.

The vibration assisted magnetic needle magnetic grinding technology can well deal with the surface defects of welded pipe fittings, especially the difficult-to-handle areas on the pipe inner surface. The oxide scale after grinding can be completely removed, and the residual stress state will also change from the original tensile stress to the compressive stress, which can effectively improve the fatigue strength and service life of the weld joints of the welded pipe fittings.

**KEY WORDS:** oxide scale, vibrating magnetic needle magnetic grinding, surface morphology, weld line, removal mechanism

焊接技术就是对焊接部位集中加热, 利用焊接材料熔化再冷却, 将 2 种或不同材料的零件连接成整体的技术<sup>[1]</sup>。焊接易造成焊接部位的不均匀, 这种不均匀性会造成零件在焊接区域出现失效、断裂等缺陷<sup>[2]</sup>。为了提高焊接部位的表面质量、抗疲劳性、耐腐蚀性<sup>[3-4]</sup>等, 众多焊接领域学者进行了大量研究。通过热处理<sup>[5-6]</sup>、化学处理<sup>[7-9]</sup>、机械处理和特种加工处理等方式对焊接零件的焊接区域进行处理, 有效提高了焊接零件的使用性能。

逯瑶等<sup>[10]</sup>利用高能喷丸技术对 7A52 铝合金焊缝进行了表面处理, 与高能喷丸前相比, 由于表面显微硬度的提高使磨损率降为原始磨损率的 29.9%, 焊接接头的使用性能得到明显提高。王宇等<sup>[11]</sup>采用表面机械研磨技术对 X80 管线钢的螺旋焊管进行了处理, 得出表面机械研磨时间越长, 塑性变形层的厚度越厚的结论, 且表面粗糙度和显微硬度均有所改善。王吉孝等<sup>[12]</sup>采用超音速微粒轰击技术对 16MnR 低合金钢

焊缝表面进行了处理, 发现经超音速微粒轰击处理后, 表层组织更均匀; 焊缝抗 H<sub>2</sub>S 应力腐蚀性能也得到了显著提高。李占明等<sup>[13]</sup>采用超声冲击技术对 2A12 铝合金焊缝进行了处理, 发现处理后焊缝中的气孔、缩松等缺陷明显减少, 焊缝表面和断面显微硬度得到明显提高, 同时消除了焊缝表面的残余拉应力<sup>[14-15]</sup>, 提高了其抗疲劳强度<sup>[16]</sup>。周留成等<sup>[17]</sup>采用激光冲击强化的方法, 大幅度提高了焊缝和热影响区的硬度, 消除了残余拉应力, 提高了焊接接头的拉伸性能, 且通过二次激光冲击强化后 12Cr2Ni4A 焊接试件的力学性能接近于新品试件。以上方法仅解决了焊缝外表面存在的一些问题, 对于管件焊缝内表面存在的一些缺陷, 用传统的加工方法并不能实现光整加工。

磁力研磨技术是近几年新发展的一种特种加工光整技术, 它属于柔性加工, 具有切削量小、质量高等特点。磁力研磨技术最早由苏联的工程师探索出来, 随后日本、韩国也开始研究磁力研磨光整加工技

术，并取得了显著的成果<sup>[18-21]</sup>。在国内，磁力研磨技术发展得较晚，主要是一些高校学者将磁力研磨技术应用于研磨平面、弯管内外表面、自由曲面等领域<sup>[18-25]</sup>。磁针磁力研磨法作为磁力研磨技术的一种，也得到了广泛应用。周传强等<sup>[26]</sup>采用磁针研磨技术对异型管件的内表面进行光整加工，使管件的表面粗糙度大幅下降，表面质量得到明显改善。陈燕等<sup>[27]</sup>利用磁针磁力研磨法去除航空发动机涡轮轴内壁的积碳，结果表明，磁针磁力研磨方法在积碳去除方面具有可行性。文中使用振动辅助磁针磁力研磨法对焊缝表面的氧化皮进行去除，突破了激光冲击、喷丸强化等技术在处理管件内表面的局限性，同时磁针磁力研磨法具有自适应性，可实现对复杂形状零件的光整加工。

## 1 管表面焊缝去除机理

采用振动辅助磁针磁力研磨法去除管表面焊缝的原理见图1。磁极盘在电机的驱动下，使磁极盘上的非导磁容器桶内的磁针绕电机的旋转轴线做回转运动，在容器桶外侧添加辅助磁极，目的是在飞跃的过程中增加磁针的飞跃高度，从而更有效地去除工件表面的氧化皮。如图2所示，在容器桶安装座的下面装有弹簧装置，启动电机后偏心块随之转动，偏心块在转动的过程中会产生离心力，在离心力的作用下容器桶就会上下、左右振动，促使磁针在旋转磁场中运动。

当磁针在旋转磁场中时，磁针会被旋转磁场磁化，使磁针变成一个小柱形磁极，会有明显的N、S极，如图3所示。对单个磁针进行受力分析，假设初始时刻梯度磁场方向与x轴方向平行，如图4a所示。

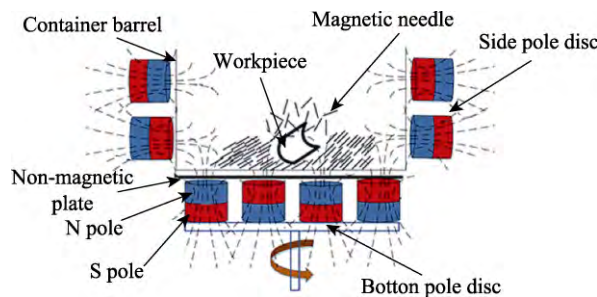


图1 加工原理  
Fig.1 Processing principle

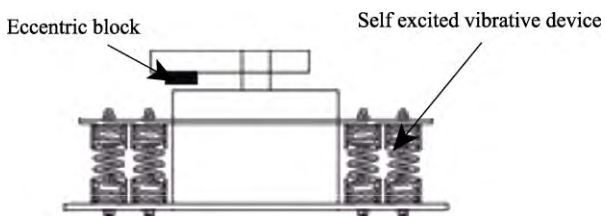


图2 自激振动装置  
Fig.2 Self excited vibration device

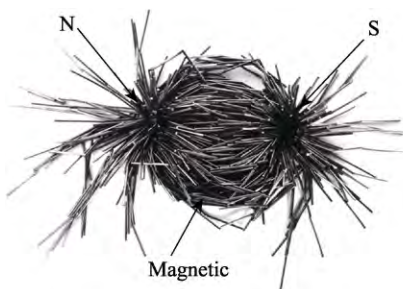


图3 磁针磁化  
Fig.3 Magnetization diagram of magnetic needle

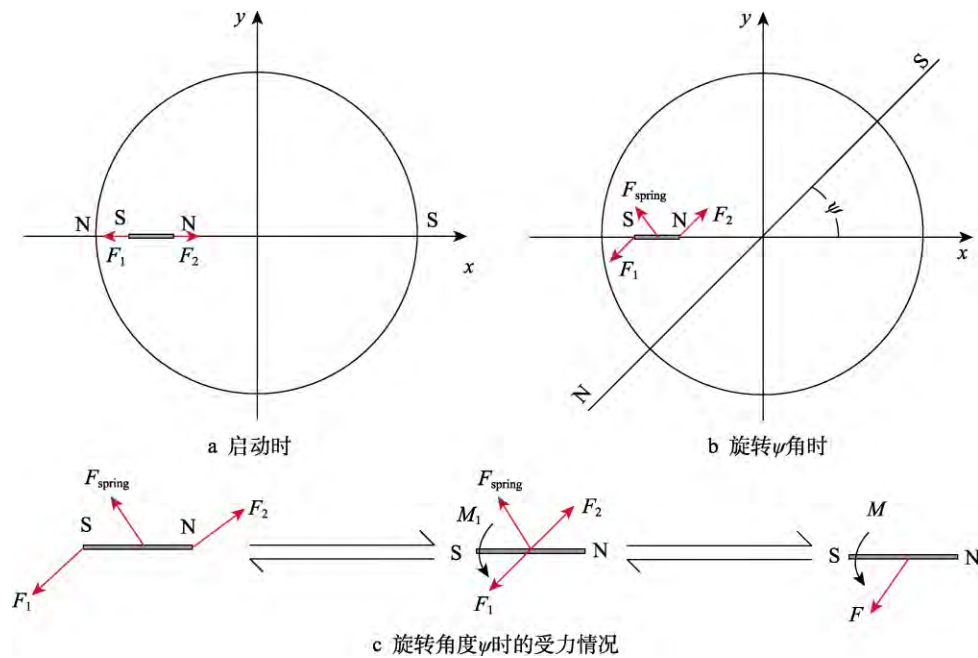


图4 单个磁针在旋转磁场中受力分析  
Fig.4 Stress analysis of single magnetic needle in rotating magnetic field: a) at startup; b) rotate  $\psi$  angular; c) force of rotation  $\psi$  angular

当磁场刚刚启动时, 根据同名磁极相互排斥、异名磁极相互吸引的原理, 此时磁针本身的 S 极与旋转磁场中的 N 极产生的吸引力  $F_1$  大于磁针本身的 N 极与旋转磁场中的 S 极产生的吸引力  $F_2$ , 即  $F_1 > F_2$ , 弹簧并无弹力, 此时磁针存在向  $x$  轴负方向移动的趋势。当旋转磁场逆时针旋转角度  $\psi$  时, 磁针在旋转磁场中的受力情况如图 4b 所示, 磁针本身的 S 极与旋转磁场中的 N 极产生的吸引力  $F_1$  大于磁针本身的 N 极与旋转磁场中的 S 极产生的吸引力  $F_2$ ,  $F_1$ 、 $F_2$  的受力方向均平行于磁场梯度方向。根据力的平移转换定理, 磁针的受力可转换为一个合力  $F$  和一个力偶  $M$ , 如图 4c 所示。

根据受力分析可知, 磁针在旋转磁场中始终受到一个斜向下的力  $F$  和一个力偶矩  $M$  的作用。在  $M$  的作用下, 使磁针在旋转磁场中绕几何中心做自转运动, 使磁针与工件发生接触, 从而达到去除毛刺的效果。在力  $F$  的作用下, 磁针与工件表面发生碰撞、划擦、翻滚, 使工件表面先发生弹性变形再发生塑性变形, 从而去除了工件表面的毛刺, 使工件表面更加光滑、平整。

单个磁针去除焊缝表面氧化皮的过程见图 5。在力  $F$  的作用下, 磁针对焊缝表面的氧化皮进行划擦, 将氧化皮逐渐从焊缝表面去除。

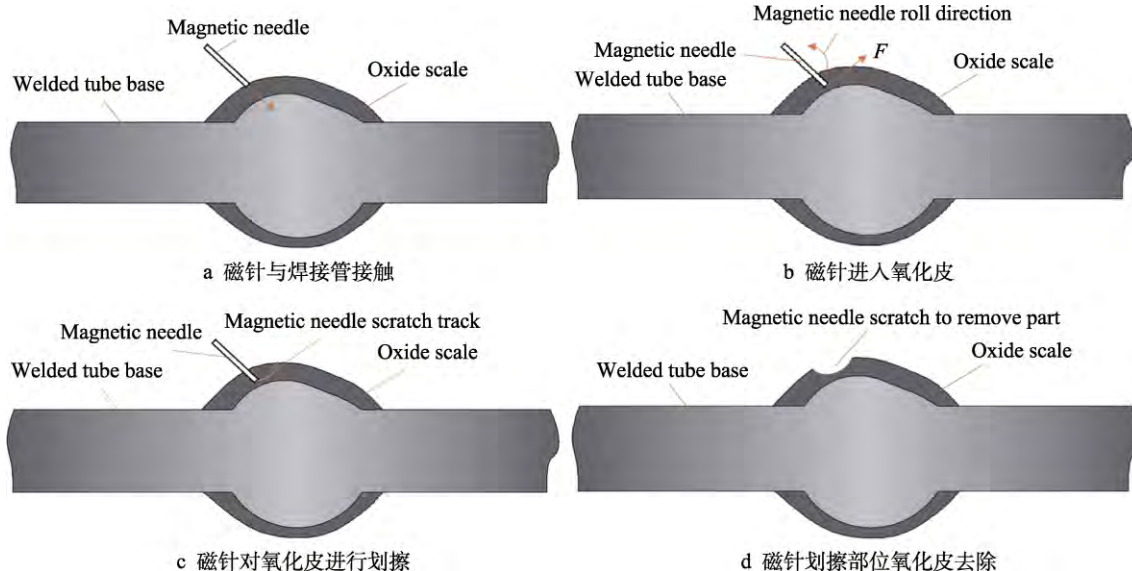


图 5 磁针去除氧化皮示意图

Fig.5 Schematic diagram of removing oxide scale by magnetic needle: a) magnetic needle is in contact with welded tube; b) schematic diagram of magnetic needle entering oxide scale; c) magnetic needle scratches oxide scale; d) removal of oxide scale at scratch part of magnetic needle

## 2 试验装置与条件

去除管表面焊缝处氧化皮的振动磁力研磨装置见图 6。将非导磁容器桶放在旋转磁极盘上方, 在磁极盘的下方安装一圈弹簧支承研磨桶座, 作为给研磨桶提供振动的源, 在研磨桶的上方安装桶盖, 防止振动频率过高时桶内研磨液和磁针飞溅。在启动电机

时, 磁极盘带动研磨桶内的磁针旋转, 在弹簧和偏心块的共同作用下, 研磨桶在竖直、水平方向上振动, 使磁针在桶内的运动更加复杂, 从而对工件表面进行全方位的研磨。

试验条件如表 1 所示。在试验过程中调节旋转磁场的频率发现, 旋转磁场的频率越高, 磁针获得的冲击力越大, 与焊缝表面的氧化皮碰撞得越频繁, 则去

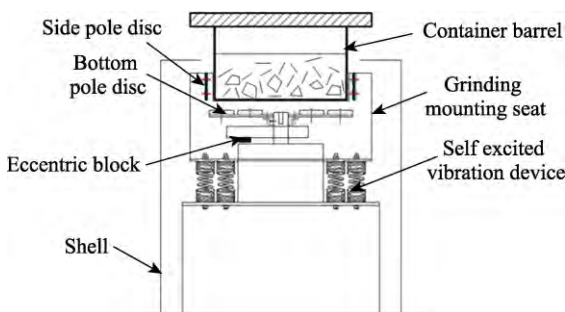


图 6 振动磁力研磨装置  
Fig.6 Schematic diagram of vibrating magnetic grinding device

表 1 试验条件  
Tab.1 Experimental conditions

Name	Experimental conditions
Iron tube/mm	35 (outer diameter), 4 (wall thickness)
Magnetic needle model/mm	$\phi 0.5 \times 5$
Magnetic needle dosage/g	400
Grinding fluid/mL	1 000
Amplitude/mm	$\pm 3$
Pole disk speed/(r·min <sup>-1</sup> )	480
Grinding time/min	40

除氧化皮的效率越高。当旋转磁场转速过高时,磁针与焊缝表面切削力过大,除了会去除表面的氧化皮外,也会划擦基体表面,从而造成焊缝表面的划伤。当研磨时间过长时,研磨液就会起到冷却、润滑的作用,对磁针去除氧化皮起到辅助作用;直径较小的磁针获得的动能不大,切削力较小,去除氧化皮的量较少,研磨效果不明显。当磁针长度较长时,磁针翻滚次数减少,对焊缝表面研磨次数较少,研磨不充分,则氧化皮的去除效果不明显。振幅不是越大越好,当振幅过大时,振动太剧烈,使得磁针飞出研磨区域,则达不到去除氧化皮的效果;当振幅过小时则达不到去除效果。表1的试验参数是经过大量试验后得出来的一组相对最优参数。

在试验过程中,采用VHX-500超景深显微镜观察焊缝研磨前后的表面形貌,利用X射线能谱分析仪(EDS)对材料微区的成分元素种类和含量进行分析,采用X射线衍射残余应力分析仪对研磨前后试验工件表面的残余应力进行检测。试验工件的实物见图7。

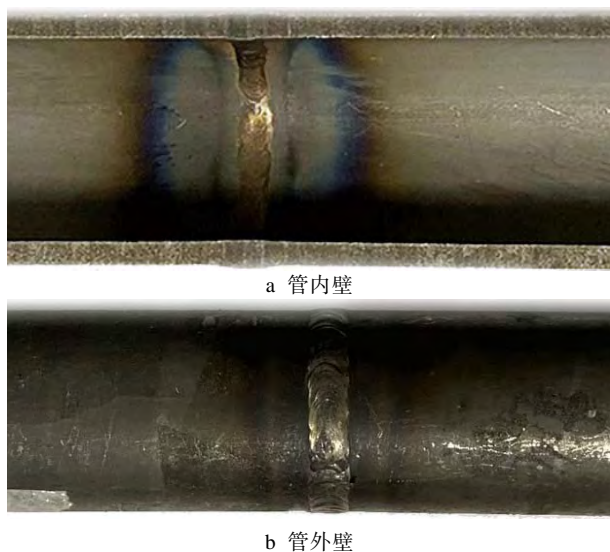


图7 试验工件

Fig.7 Schematic diagram of experimental workpiece:  
a) inner wall of pipe; b) outer wall of pipe

### 3 结果与分析

#### 3.1 焊缝去除情况

研磨前管件内表面焊缝的表面形貌见图8a,可见焊缝表面存在大量的氧化皮,颜色发黑。采用无振动辅助磁针磁力研磨去除焊缝表面氧化皮后的焊缝表面形貌见图8b,可见氧化皮得到一定程度的去除,但在表层凹坑内仍有少量残留,且表面明显凹凸不平。利用振动辅助磁针磁力研磨去除焊缝表面氧化皮后的表面形貌见图8c,焊缝表面基本看不见氧化皮,颜色发亮,很好地改善了表面质量。在加工条件相同的情况下,有振动辅助的磁力研磨效果比无振动辅助的研磨效果好,去除表面氧化皮的量更多,效率更高。

#### 3.2 焊缝氧化皮去除结果验证

利用超景深电子显微镜观察焊接管件焊缝处的表面形貌可了解氧化皮的去除情况,利用X射线能谱分析仪(EDS)对加工前后的焊接管内壁进行元素成分分析,可以进一步从成分上论证氧化皮是否被完全去除。

与非导磁类管件相比,利用磁力研磨加工技术在加工导磁性焊接管件方面更加困难,因此选择具有良好导磁性能的焊接管件进行研磨前后的加工效果对比和元素分析更具有普遍性。在扫描电子显微镜下,不同状态管件焊缝表面的微观形貌见图9。首先,将管件切开,对切面的元素成分进行定量分析,得到了管件基体的元素成分。然后,对焊接后未经处理的焊接管内壁原始焊缝表面进行成分分析,得到焊接管内壁氧化皮的原有成分。最后,对加工不同时间后的焊接管内壁焊缝表面进行成分分析。相应标记区域的EDS能谱图见图10,由于管件基体的元素成分与管件焊缝处未经处理的表面元素成分在加工前后变化最为明显的是C、Fe等2种元素,所以选用C和Fe元素进行加工前后的对比,以验证振动辅助磁针磁力研磨技术是否可以完全去除焊接管内壁焊缝表面的氧化皮成分。

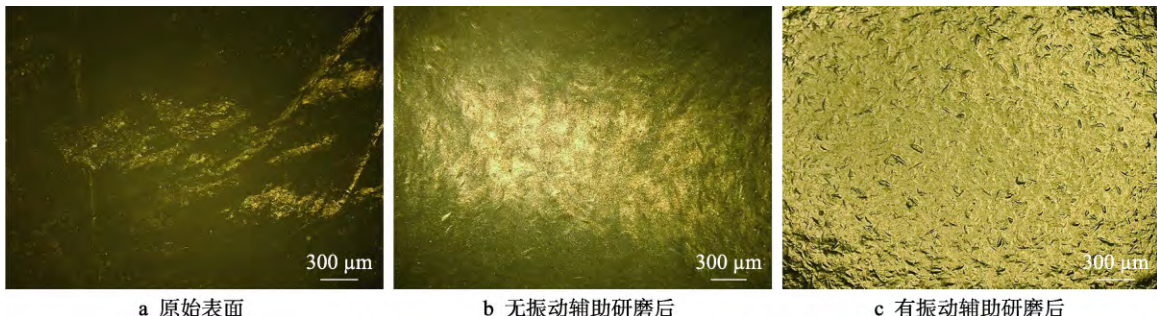


图8 有无振动辅助研磨的表面形貌对比

Fig.8 Comparison of surface morphology of welded tubes with or without vibration assisted grinding: a) original surface; b) after no vibration assisted grinding; c) after vibration assisted grinding

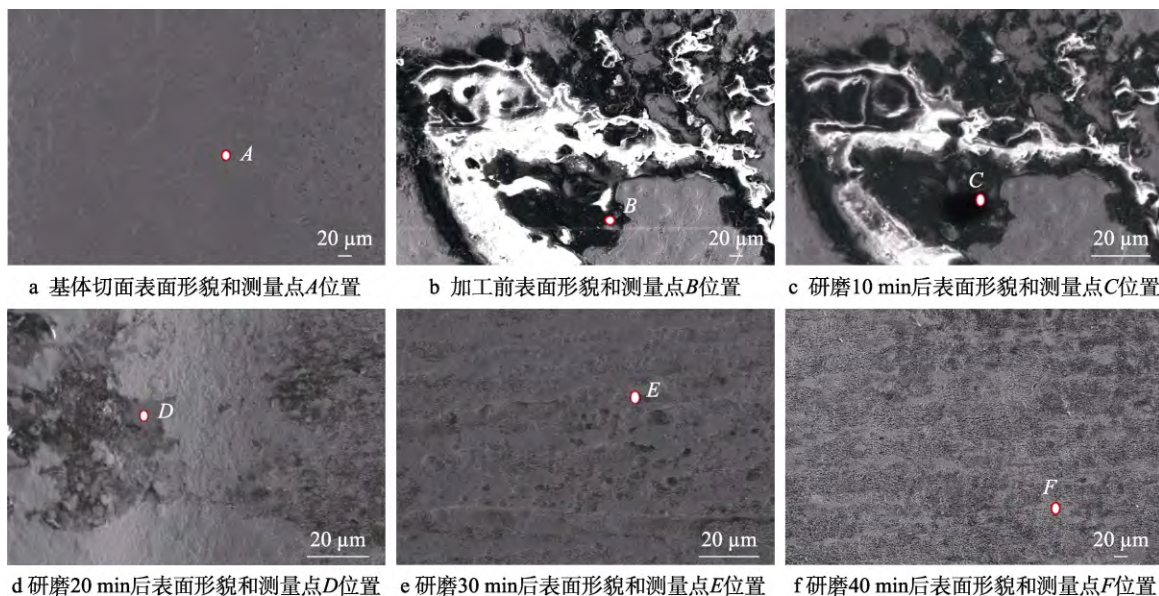


图 9 表面形貌与测量点位置

Fig.9 Surface topography and location of measurement points: a) surface topography and measurement points A of the cut surface of the substrate; b) original surface topography and measurement point B; c) surface topography after 10min and point C; d) surface topography after 20 min and point D; e) surface topography after 30 min and point E; f) surface topography after 40 min and point F

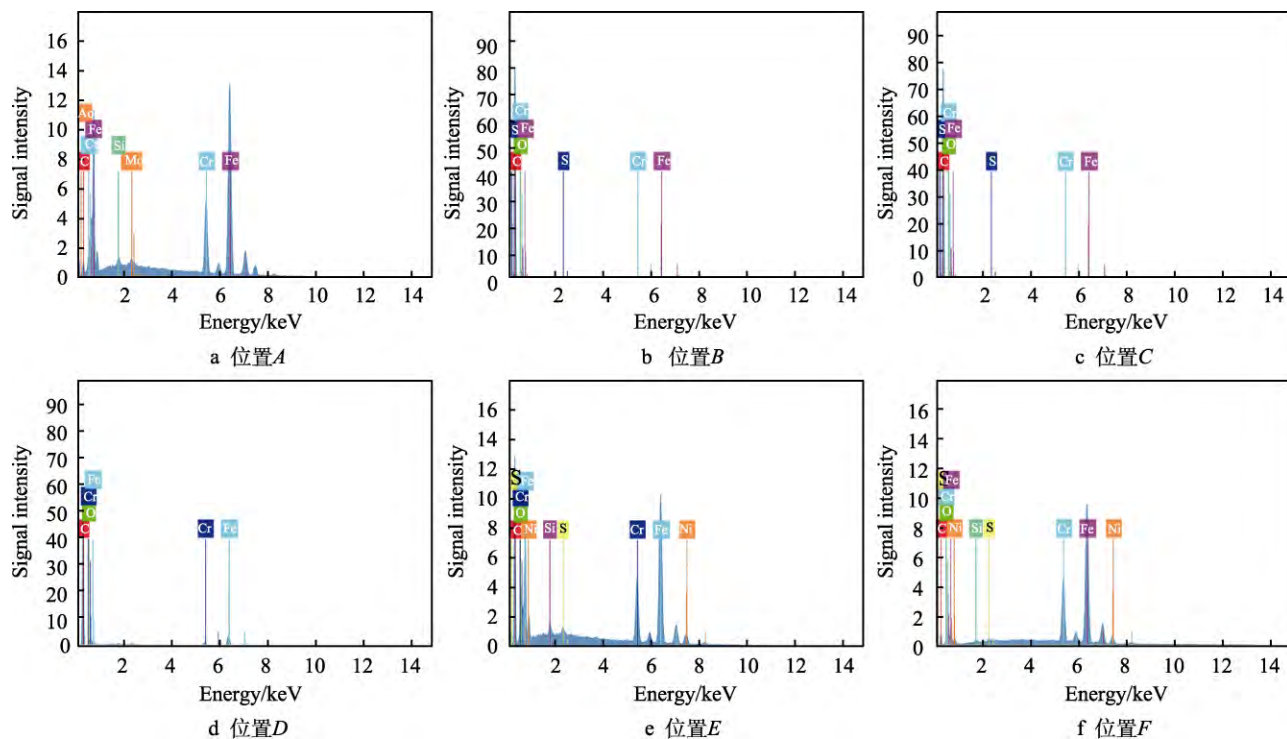


图 10 不同测量点的能量谱

Fig.10 Energy spectrum of different measurement points: a) point A; b) point B; c) point C; d) point D; e) point E; f) point F

对未经处理的焊接管焊缝处表面的元素成分进行了检测, 将检测出的元素成分作为焊缝处存在的氧化皮元素组成。从表 2 可以看出, 焊接管基体与焊缝表面处氧化皮的成分主要在 C 和 Fe 等 2 种元素的含量上存在较明显的差异。其中, 氧化皮中 C、Fe 元素的质量分数分别为 88.62%、0.45%; 焊接管基体中 C、Fe 元素的质量分数分别为 2.98%、67.09%; 经过振动

辅助磁针磁力研磨技术加工后, 焊接管表面 C、Fe 元素的质量分数分别为 3.10%、63.51%。加工后管表面的元素含量与基体的元素含量基本相同, 对比加工前后的表面形貌也没发现明显的氧化皮残留, 说明氧化皮被去除干净。

通过以上分析可知, 采用振动辅助磁力研磨可以完全去除焊缝表面的氧化皮, 同时也验证了表面形貌

表2 不同位置元素的质量分数

Tab.2 Mass percentages of elements in different positions  
wt. %

Element	C	O	S	Cr	Fe	Mo	Si	Ni
A position	2.98	—	—	13.63	67.09	1.01	0.49	—
B position	88.62	10.76	0.05	0.11	0.45	—	—	—
C position	29.24	5.03	0.02	0.13	0.18	—	—	—
D position	23.27	2.93	—	0.43	1.55	—	—	—
E position	11.2	2.05	0.15	1.03	4.04	—	0.17	0.70
F position	3.10	0.5	0.19	14.18	63.51	—	0.62	2.39

Note: “—” in the table indicates that this element is not detected.

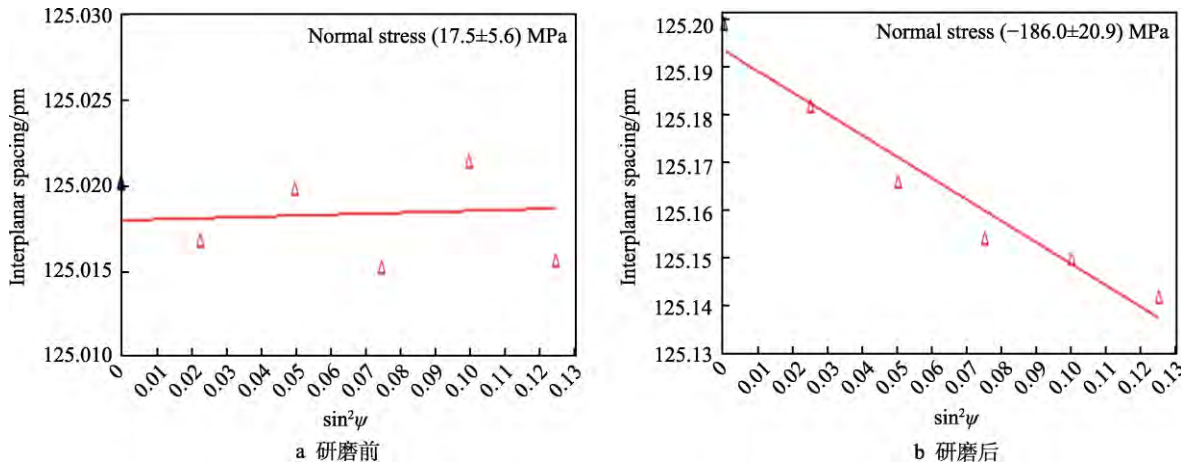


图11 焊缝表面研磨前后残余应力

Fig.11 Residual stress diagram of weld surface before and after grinding: a) before grinding; b) after grinding

## 4 结论

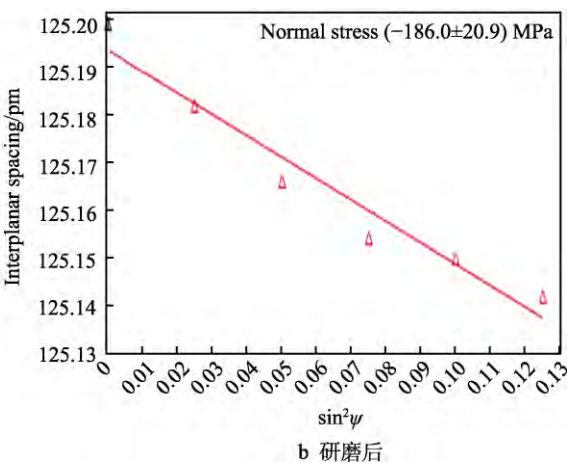
通过对研磨前后焊缝表面形貌进行观测可以看出,采用振动辅助磁针磁力研磨工艺加工后管件焊缝表面的颜色由暗变亮,焊缝处无明显氧化皮存在,焊缝表面的残余应力由原始的拉应力(17.5 MPa)变为压应力(186.0 MPa),有效地提高了焊缝的抗疲劳强度和使用寿命。对振动辅助磁针磁力研磨前后焊缝表面处的成分检测分析与对比发现,加工前后焊缝表面的C元素含量降低了85.52%,Fe元素含量增加了63.06%,加工后焊接管表面元素与基体元素大体相同,可见氧化皮被去除得较彻底。

## 参考文献:

- [1] 滕诚信,左松,赵琨,等.焊接接头表面改性的研究进展[J].表面技术,2014,43(4): 149-157.  
TENG Cheng-xin, ZUO Song, ZHAO Kun, et al. Progress in Surface Modification of Welded Joints[J]. Surface Technology, 2014, 43(4): 149-157.
- [2] 孙朋飞,姚丹丹,张鹏林,等.金属焊接接头疲劳寿命延长技术综述[J].材料导报,2021,35(9): 9059-9068.  
SUN Peng-fei, YAO Dan-dan, ZHANG Peng-lin, et al. Fatigue Life Extension Technologies for Weld Joints of Metals: A Review[J]. Materials Reports, 2021, 35(9): 9059-9068.

分析的结论。

焊接管的焊接过程属于局部不均匀加热的过程,在这个过程中会产生大量的热量,导致金属的状态和显微组织的变化,焊接管在加热冷却过程中会产生残余应力。焊接管在使用过程中由于内部残余应力的存在更容易产生裂纹,从而造成零件的损坏。通过X射线衍射仪检测研磨前后的残余应力可知(见图11),在加工前焊缝处的残余应力为17.5 MPa,经过振动辅助磁针磁力研磨加工后残余应力变为-186.0 MPa,残余应力得到大幅降低,有效地提高了焊缝处的抗疲劳强度和使用寿命。



SUN Peng-fei, YAO Dan-dan, ZHANG Peng-lin, et al. Fatigue Life Extension Technologies for Weld Joints of Metals: A Review[J]. Materials Reports, 2021, 35(9): 9059-9068.

[3] 赵兵兵,张慧霞,贾瑞灵,等.低合金钢焊接接头腐蚀性能研究进展[J].装备环境工程,2013,10(6): 60-64.

ZHAO Bing-bing, ZHANG Hui-xia, JIA Rui-ling, et al. Research Progress on the Corrosion Behavior of Low Alloy Steel Weldments[J]. Equipment Environmental Engineering, 2013, 10(6): 60-64.

[4] 贾思洋,李超,韩东锐.B610E不同焊接接头在石油沉积水中的耐蚀性研究[J].装备环境工程,2012,9(6): 25-28.

JIA Si-yang, LI Chao, HAN Dong-rui. Study on Corrosion-Resistant Performance of Different Welded Joints of B610E in the Deposited Water of Petroleum[J]. Equipment Environmental Engineering, 2013, 9(6): 25-28.

[5] 徐峰,李文虎,艾桃桃,等.Q235钢表面氩弧熔覆TiC复合涂层的组织与性能[J].表面技术,2012,41(5): 53-55.

XU Feng, LI Wen-hu, AI Tao-tao, et al. The Microstructure and Property of TiC Composite Coating Deposited by Argon Arc Cladding on Q235 Steel Surface[J]. Surface Technology, 2012, 41(5): 53-55.

- [6] 曹艳, 李涌泉, 褚芳芳. 45 钢表面 Ni20 合金激光熔覆层的组织及抗高温氧化性能[J]. 表面技术, 2012, 41(3): 54-56.  
CAO Yan, LI Yong-quan, CHU Fang-fang. Microstructure and High Temperature Oxidation Resistance of Laser Cladding Ni20 Alloy on 45 Steel[J]. Surface Technology, 2012, 41(3): 54-56.
- [7] 闻勃, 郭兴伍, 陈洁, 等. 2024 铝合金表面微弧氧化及封孔处理对其疲劳性能的影响[J]. 表面技术, 2012, 41(5): 14-16.  
WEN Bo, GUO Xing-wu, CHEN Jie, et al. Effect of Micro-arc Oxidation Coatings and Micro-arc Oxidation Coatings after Sealing Treatment on Fatigue Properties of 2024 Aluminum Alloys[J]. Surface technology, 2012, 41(5): 14-16.
- [8] 李旭东, 穆志韬, 刘治国, 等. LY12CZ 航空铝合金腐蚀疲劳断口研究[J]. 装备环境工程, 2013, 10(4): 9-12.  
LI Xu-dong, MU Zhi-tao, LIU Zhi-guo, et al. Corrosion Fatigue Fracture Analysis of LY12CZ Aluminum Alloy[J]. Equipment Environmental Engineering, 2013, 10(4): 9-12.
- [9] 王雁涛, 杨钿. 铝合金结构件应力腐蚀裂纹机理分析[J]. 装备环境工程, 2013, 10(1): 53-56.  
WANG Yan-tao, YANG Dian. Analysis on Stress Corrosion Crack Mechanisms of Aluminum Alloy Structure[J]. Equipment Environmental Engineering, 2013, 10(1): 53-56.
- [10] 逯瑶, 陈芙蓉, 解瑞军. 7A52 铝合金焊接接头表面纳米化前后的性能分析[J]. 焊接学报, 2011, 32(1): 57-60.  
LU Yao, CHEN Fu-rong, XIE Rui-jun. Properties of 7A52 Aluminum Alloy Welded Joint before and after Surface Nanocrystallization[J]. Transactions of The China Welding Institution, 2011, 32(1): 57-60.
- [11] 王宇, 黄敏, 高惠临, 等. 表面机械研磨处理对 X80 管线钢焊接接头组织与性能的影响[J]. 机械工程材料, 2009, 33(8): 50-53.  
WANG Yu, HUANG Min, GAO Hui-lin, et al. Influence of Surface Mechanical Attrition Treatment on Microstructure and Properties of X80 Pipeline Steel Welded Joints [J]. Materials for Mechanical Engineering, 2009, 33(8): 50-53.
- [12] 王吉孝, 王志平, 霍树斌, 等. 16MnR 钢焊接接头表面纳米化及接头抗 H<sub>2</sub>S 应力腐蚀性能[J]. 焊接, 2005(2): 13-16.  
WANG Ji-xiao, WANG Zhi-ping, HUO Shu-bin, et al. Surface Nanocrystallization of 16MnR Low Alloy Steel Welded Joints and Investigation on Resisting H<sub>2</sub>S Stress Corrosion of Welded Joint[J]. Welding & Joining, 2005(2): 13-16.
- [13] 李占明, 朱有利, 王侃, 等. 2A12 铝合金焊接接头超声冲击强化机理分析[J]. 焊接学报, 2008, 29(9): 55-58.  
LI Zhan-ming, ZHU You-li, WANG Kan, et al. Analysis of Strengthening Mechanism of Ultrasonic Impact Treatment of 2A12 Aluminum Alloy Weld Joint[J]. Transactions of The China Welding Institution, 2008, 29(9): 55-58.
- [14] 朱有利, 李占明, 何嘉武, 等. 超声冲击处理 2A12 铝合金焊缝表层微观组织结构变化[J]. 材料工程, 2009, 37(7): 79-82.  
ZHU You-li, LI Zhan-ming, HE Jia-wu, et al. Microstructure Changes of 2A12 Aluminum Alloy Weld Bead Surface Layer by Ultrasonic Impact Treatment[J]. Journal of Materials Engineering, 2009, 37(7): 79-82.
- [15] 朱有利, 李占明, 韩志鑫, 等. 超声冲击处理对 2A12 铝合金焊接接头表层组织性能的影响[J]. 稀有金属材料与工程, 2010, 39(S1): 130-133.  
ZHU You-li, LI Zhan-ming, HAN Zhi-xin, et al. Effect of Ultrasonic Impact Treatment on Microstructure and Properties of Surface Layer of 2A12 Aluminum Alloy Weld Joint[J]. Rare Metal Materials and Engineering, 2010, 39(S1): 130-133.
- [16] 李占明, 朱有利, 王侃. 超声冲击处理对 2A12 铝合金焊接接头组织的影响[J]. 金属热处理, 2008, 33(7): 53-56.  
LI Zhan-ming, ZHU You-li, WANG Kan. Influence of Ultrasonic Impact Treatment on Microstructure of 2A12 Aluminum Alloy Welded Joint[J]. Heat Treatment of Metals, 2008, 33(7): 53-56.
- [17] 周留成, 周磊, 李应红, 等. 激光冲击强化对不锈钢焊接接头拉伸性能的影响[J]. 焊接学报, 2011, 32(4): 52-54.  
ZHOU Liu-cheng, ZHOU Lei, LI Ying-hong, et al. Effect of Laser Shock Processing on Tensile Strength of Welded Joints[J]. Transactions of The China Welding Institution, 2011, 32(4): 52-54.
- [18] 杨海吉, 陈燕, 金文博, 等. 球形磁极在小直径钛合金管内表面抛光中的应用[J]. 组合机床与自动化加工技术, 2018(7): 145-147.  
YANG Hai-ji, CHEN Yan, JIN Wen-bo, et al. Application of Spherical Magnetic Pole in Polishing of Inner Surface of Small Diameter TC4 Tubes[J]. Modular Machine Tool & Automatic Manufacturing Technique, 2018(7): 145-147.
- [19] 张志超. 细微零件精密研磨机的设计及试验研究[D]. 鞍山: 辽宁科技大学, 2016: 1-6.  
ZHANG Zhi-chao. Tiny Parts Precision Grinding Machine Design and Experimental Research[D]. Anshan: University of Science and Technology Liaoning, 2016: 1-6.
- [20] 徐宗贵. 简式永磁抛光机的工作原理和应用研究[D]. 鞍山: 辽宁科技大学, 2014: 1-2.  
XU Zong-gui. Research of Permanent Magnetic Mill Working Principle and Application[D]. Anshan: University of Science and Technology Liaoning, 2014: 1-2.
- [21] MORI T, HIROTA K, KAWASHIMA Y. Clarification of Magnetic Abrasive Finishing Mechanism[J]. Journal of Materials Processing Technology, 2003, 143/144: 682-686.

(下转第 459 页)

浸润性分析及设计[J]. 化学学报, 2019, 77(3): 269-277.  
MA Guo-jia, ZHENG Hai-kun, CHANG Shi-nan, et al. Wettability Analysis and Design of Micro-Nanostructured Superhydrophobic Surface[J]. Acta Chimica Sinica, 2019, 77(3): 269-277.

[27] JIANG Shu-yue, ZHANG Hai-feng, JIANG Chun-feng, et al. Antifrosting Performance of a Superhydrophobic Surface by Optimizing the Surface Morphology[J]. Langmuir: the ACS Journal of Surfaces and Colloids, 2020, 36(34): 10156-10165.

(上接第 380 页)

- [20] XIA Yun-qing, HE Yi, CHEN Chun-lin, et al. MoS<sub>2</sub> Nanosheets Modified SiO<sub>2</sub> to Enhance the Anticorrosive and Mechanical Performance of Epoxy Coating[J]. Progress in Organic Coatings, 2019, 132: 316-327.
- [21] HU Shi-hao, MUHAMMAD M, WANG Meng-zhe, et al. Corrosion Resistance Performance of Nano-MoS<sub>2</sub>-Containing Zinc Phosphate Coating on Q235 Steel[J]. Materials Letters, 2020, 265: 127256.
- [22] CHEN Chun-lin, HE Yi, XIAO Guoqing, et al. Two-Dimensional Hybrid Materials: MoS<sub>2</sub>-RGO Nanocomposites Enhanced the Barrier Properties of Epoxy Coating [J]. Applied Surface Science, 2018, 444: 511-521.

[23] 赵鹏飞, 宋喜梅, 张海琛, 等. 碳纳米管与二硫化钼协同增强丁腈橡胶复合材料吸波性能[J]. 高分子材料科学与工程, 2021, 37(4): 174-181.

Zhao Peng-fei, Song Xi-mei, Zhang Hai-chen, et al. Synergistic Effects of Molybdenum Disulfide and Multiwalled Carbon Nanotubes on the Microwave Absorbing Performance of Nitrile Butadiene Rubber Composites[J]. Polymer Materials Science & Engineering, 2021, 37(4): 174-181.

[24] ZHANG Guo-zhu, QIN Shu-yang, YAN Long-ge, et al. Simultaneous Improvement of Electromagnetic Shielding Effectiveness and Corrosion Resistance in Magnesium Alloys by Electropulsing[J]. Materials Characterization, 2021, 174: 111042.

(上接第 407 页)

- [22] 谭悦, 陈燕, 曾加恒, 等. 电解-磁力复合研磨 TA18 钛合金管内表面研究[J]. 组合机床与自动化加工技术, 2018(2): 140-142.
- TAN Yue, CHEN Yan, ZENG Jia-heng, et al. Study on Inner Surface of TA18 Titanium Alloy Pipe by Electrochemical Magnetic Composite Finishing[J]. Modular Machine Tool & Automatic Manufacturing Technique, 2018(2): 140-142.
- [23] JAIN V K, SAREN K K, RAGHURAM V, et al. Force Analysis of Magnetic Abrasive Nano-Finishing of Magnetic and Non-Magnetic Materials[J]. The International Journal of Advanced Manufacturing Technology, 2019, 100(5): 1137-1147.
- [24] LIU Z Q, CHEN Y, LI Y J, et al. Comprehensive Performance Evaluation of the Magnetic Abrasive Particles [J]. The International Journal of Advanced Manufacturing Technology, 2013, 68(1): 631-640.

[25] LIN C T, YANG L D, CHOW H M. Study of Magnetic Abrasive Finishing in Free-Form Surface Operations Using the Taguchi Method[J]. The International Journal of Advanced Manufacturing Technology, 2007, 34(1): 122-130.

[26] 周传强, 韩冰, 马学东, 等. SUS316 异形管件内表面磁针磁力研磨的试验研究[J]. 现代制造工程, 2019(10): 1-5.

ZHOU Chuan-qiang, HAN Bing, MA Xue-dong, et al.

Study on the Magnetic Abrasive Finishing of the Inner Surface of SUS316 Irregular Tubular by Magnetic Needles [J]. Modern Manufacturing Engineering, 2019(10): 1-5.

[27] 陈燕, 胡玉刚, 巫昌海, 等. 磁针磁力研磨去除涡轮轴内壁积碳[J]. 表面技术, 2020, 49(6): 259-266.

CHEN Yan, HU Yu-gang, WU Chang-hai, et al. Removal of Carbon Deposition on the Inner Wall of Turbo Shaft by Magnetic Needle Grinding[J]. Surface Technology, 2020, 49(6): 259-266.

责任编辑: 彭颖

(上接第 451 页)

- [36] KAMDEM D P, RIEDL B, ADNOT A, et al. ESCA Spectroscopy of Poly(Methyl Methacrylate) Grafted Onto Wood Fibers[J]. Journal of Applied Polymer Science, 1991, 43(10): 1901-1912.
- [37] POPESCU C M, TIBIRNA C M, VASILE C. XPS Characterization of Naturally Aged Wood[J]. Applied Surface Science, 2009, 256(5): 1355-1360.
- [38] VENKATESWARA RAO A, KULKARNI M M, AMALNERKAR D P, et al. Superhydrophobic Silica Aerogels Based on Methyltrimethoxysilane Precursor[J]. Journal of Non-Crystalline Solids, 2003, 330(1/2/3): 187-195.
- [39] SHAFRIN E G, ZISMAN W A. Constitutive Relations in the Wetting of Low Energy Surfaces and the Theory of

the Retraction Method of Preparing Monolayers[J]. The Journal of Physical Chemistry, 1960, 64(5): 519-524.

[40] ZHANG Yang, XU De-liang, MA Li-bo, et al. Influence of Heat Treatment on the Water Uptake Behavior of Wood[J]. BioResources, 2017, 12(1): 1697-1705.

[41] 方露, 王正, 熊先青. 热压温度对硅烷化木单板/聚乙烯薄膜复合材料性能的影响[J]. 浙江农林大学学报, 2016, 33(3): 483-488.

FANG Lu, WANG Zheng, XIONG Xian-qing. Properties of Silane Modified Poplar Veneer/High Density Polyethylene Film Composites with Varying Pressing Temperatures[J]. Journal of Zhejiang A & F University, 2016, 33(3): 483-488.

责任编辑: 彭颖